Supplemental Materials and Methods

Reagents

AAV-Flex-Chronos-GFP, AAV-CAG-flex-GFP [1], and retrograde AAVretro-CAG-tdTomato were purchased from the University of North Carolina Vector Core. All reagents were obtained from Sigma except DNQX (Abcam) and APV (R&D Systems).

Animals

Drd1a-Cre (D1-Cre) and *Drd2*-Cre (D2-Cre) mice were obtained from the Mutant Mouse Regional Resource Center. Ai32, Ai14, and Snap25 mice were purchased from the Jackson Laboratory. D1-Cre and D2-Cre mice were crossed with Ai32, Ai14, or Snap25 mice to obtain D1-Cre;Ai32, D2-Cre;Ai32, D1-Cre;Ai14, D2-Cre;Ai14, D1-Cre;Snap25, and D2-Cre;Snap25 mice. Mouse genotypes were determined by PCR analysis of Cre or the fluorescent protein in tail DNA (Cre for D1-Cre and D2-Cre mice; EYFP for Ai32 mice; tdTomato for Ai14 mice; GFP for Snap25 mice) [2, 3]. Male mice (3-6 months-old) were used in this study. Mice were housed in a temperature- and humidity-controlled vivarium with a 12-h light/dark cycle (lights on at 11:00 P.M.). Food and water were available *ad libitum*. All animal care and experimental procedures were approved by the Texas A&M University Institutional Animal Care and Use Committee.

Stereotaxic infusion

The viral infusion procedure has been described previously [3]. Animals were anesthetized with 3-4% isoflurane at 1.0 L/min and mounted in a stereotaxic surgery frame. The head was leveled and craniotomy was performed using stereotaxic coordinates adapted from the mouse brain atlas [4]. AAV-Flex-Chronos-GFP (Figure 5)

or AAV-CAG-Flex-GFP (Figure S1) was bilaterally infused at the mPFC of D1-Cre;Ai14 and D2-Cre;Ai14 mice (AP, +1.94 mm; ML, ±0.25 mm; DV, -2.5 mm from the Bregma). AAVretro-CAG- Tdtomato was bilaterally infused into the DMS (AP1, +1.18 mm; ML1, ±1.3 mm; DV1, -2.9 mm; AP2, +0.38 mm; ML2, ±1.67 mm; DV2, -2.9 mm from the Bregma) of D1-/D2Cre;Snap25 mice. A volume of 0.3 µL/site (mPFC) and 0.5 µL/site (DMS) of the virus was infused at a rate of 0.1 µL/min. The injectors were left in place for an additional 5-10 min before removal. The scalp incision was then sutured, and the animals were returned to their home cage for recovery.

Intermittent-access to 20% alcohol two-bottle-choice drinking procedure

To establish high levels of alcohol consumption in mice, we utilized the intermittent-access to 20% alcohol two-bottle-choice drinking procedure [2, 3, 5, 6]. D1-Cre;Ai32, D2-Cre;Ai32, and D2-Cre;Ai14 mice were given three 24-h sessions per week (Mondays, Wednesdays, and Fridays) of free access to two bottles containing water or 20% alcohol, with 24-h and 48-h withdrawal periods (Tuesdays, Thursdays, Saturdays, and Sundays). During the withdrawal periods, the mice had access to two bottles of water. The placement of the alcohol bottle was alternated for each drinking session to control for side preferences. Control animals were treated in the same manner, except that they were presented with water only. This procedure was followed for 8 weeks.

Electrophysiology

Slice preparation and electrophysiology recording have been described previously [3, 5, 7-9].

Slice preparation. Animals were euthanized and 250-μm coronal sections containing the DMS or mPFC (Figure S1) were prepared in an ice-cold cutting solution containing (in mM): 40 NaCl, 148.5 sucrose, 4 KCl, 1.25 NaH_2PO_4, 25 $NaHCO_3$, 0.5 $CaCl_2$, 7 $MgCl_2$, 10 glucose, 1 sodium ascorbate, 3 sodium pyruvate, and 3 myo-inositol saturated with 95% O_2 and 5% CO_2. Striatal slices from alcohol-drinking mice were prepared twenty-four hours or nine days after the last alcohol-drinking session. Slices were then incubated in a 1:1 mixture of the cutting solution and external solution at 32°C for 45 min. The external solution was composed of the following (in mM): 125 NaCl, 4.5 KCl, 2.5 $CaCl_2$, 1.3 $MgCl_2$, 1.25 NaH_2PO_4, 25 $NaHCO_3$, 15 glucose, and 15 sucrose saturated with 95% O_2 and 5% CO_2. Slices were then maintained in the external solution at room temperature until use.

Whole-cell recordings. All recordings were conducted at 32°C and perfused with the external solution at a rate of 2-3 mL/min. Picrotoxin (100 μM) was included in the external solution of all recordings to block $GABA_A$ receptor-mediated transmission. Fluorescent axonal fibers and neurons were visualized using an epifluorescent microscope (Examiner A1, Zeiss). D1- and D2-MSNs of D2-Cre;Ai14 mice, mPFC neurons of D1-/D2-Cre;Ai14 mice were identified by fluorescence of tdTomato. A biophysical approach was used to distinguish D1- and D2-MSNs in D1-Cre;Ai32 or D2-Cre;Ai32 mice (see Figure S1A-S1C for details). MSNs were clamped at -70 mV. The pipette solution contained (in mM): 119 $CsMeSO_4$, 8 tetraethylammonium chloride, 15 4-(2-hydroxyethyl) pipera- zine-1-ethanesulfonic acid (HEPES), 0.6 ethylene glycol tetra- acetic acid (EGTA), 0.3 Na_3GTP, 4 MgATP, 5 QX-314, and 7 phosphocreatine, with an osmolarity of ~280 mOsm/L. The pH was adjusted to 7.3 with CsOH. For selective stimulation of inputs from channelrhodopsin-expressing fibers onto DMS neurons, 470-nm light was delivered

through the objective lens for 2 ms. To generate input-output curves for AMPA receptor (AMPAR)-mediated excitatory postsynaptic currents (EPSCs), currents generated in response to stimulation at increasing intensities were recorded. The paired-pulse ratio (PPR) was calculated using two EPSCs that were activated by paired two optical stimulation delivered at 50 or 100 ms apart. In recordings where Ca^{2+} was replaced with Sr^{2+}, AMPAR-mediated quantal events were collected during 50-500 ms after each stimulus (delivered once every 30 s) in an external solution containing APV (50 μM), 2.5 mM Sr^{2+}, and 0 Ca^{2+} [10, 11]. Quantal events were analyzed using MiniAnalysis software (Synaptosoft) with detection parameters set at > 5 pA amplitude. For each cell, at least 30 trials were taken.

mPFC neurons were clamped at -60 mV with electrodes containing (in mM): 123 potassium gluconate, 10 HEPES, 0.2 EGTA, 8 NaCl, 2 MgATP, 0.3 NaGTP, pH 7.2-7.3, corresponding to an osmolarity of ~280 mOsm. mPFC cells with red fluorescence were recorded in the presence of DNQX (10 μM), APV (50 μM), and picrotoxin (100 μM) to block both excitatory and inhibitory synaptic transmission. A 500-ms current step was injected every minute to evoke firing. The baseline excitability was maintained for 5 min before D1 agonist or D2 agonist application for 10 min. Baseline firing was calculated from 1 to 5 minutes, and post-agonist (D1 or D2) firing was averaged from 11 to 15 minutes.

Histology and Cell Counting

Mice were intracardially perfused with 4% paraformaldehyde in phosphate-buffered saline. The brains were removed and post-fixed overnight in 4% paraformaldehyde at 4°C prior to dehydration in a 30% sucrose solution. The brains were cut into 50-μm coronal or

sagittal sections using a cryostat. The sections (Figure 1A, 1B, 5B, and 5C) were stained with NeuroTrace Red or NeuroTrace Blue (1:100). Fluorescent images were acquired using a confocal microscope (FluoView 1200, Olympus, Tokyo, Japan) and analyzed using IMARIS 8.3.1 (Bitplane, Zürich, Switzerland), as previously reported (Wei et al., 2017; Cheng et al., 2017). Cell counting was performed in 12 double transgenic mice (Figure 2, D1-Cre;Snap25 and D2-Cre;Snap25; Figure S2, D1-Cre;Ai14 and D2-Cre;Ai14). In each brain region, a total of 33-35 brain sections were imaged from each mouse. Counting of green and red neurons were conducted using Imaris 8.3.1, which also calculated co-localization [2].

Statistical analysis

All data are expressed as the mean ± the standard error of the mean. Differences were considered to be statistically significance if $p < 0.05$. Statistical analysis was conducted by SigmaPlot.

Supplementary Table 1. Comparison of levels of alcohol consumption in transgenic mice used.

Mouse lines	Alcohol intake (g/kg/24h)	
D2-Cre;Ai14	19.97 ± 3.24	n = 5
D1-Cre;Ai32	19.14 ± 2.31	n = 7
D2-Cre;Ai32	19.22 ± 1.88	n = 11

All mice were exposed to alcohol using the intermittent access to 20% alcohol 2-bottle-choice drinking procedure. The levels of alcohol intake were the averaged values of the last 3 drinking sessions. There was no significant difference in alcohol intake among mouse lines; $p > 0.05$, one-way ANOVA.

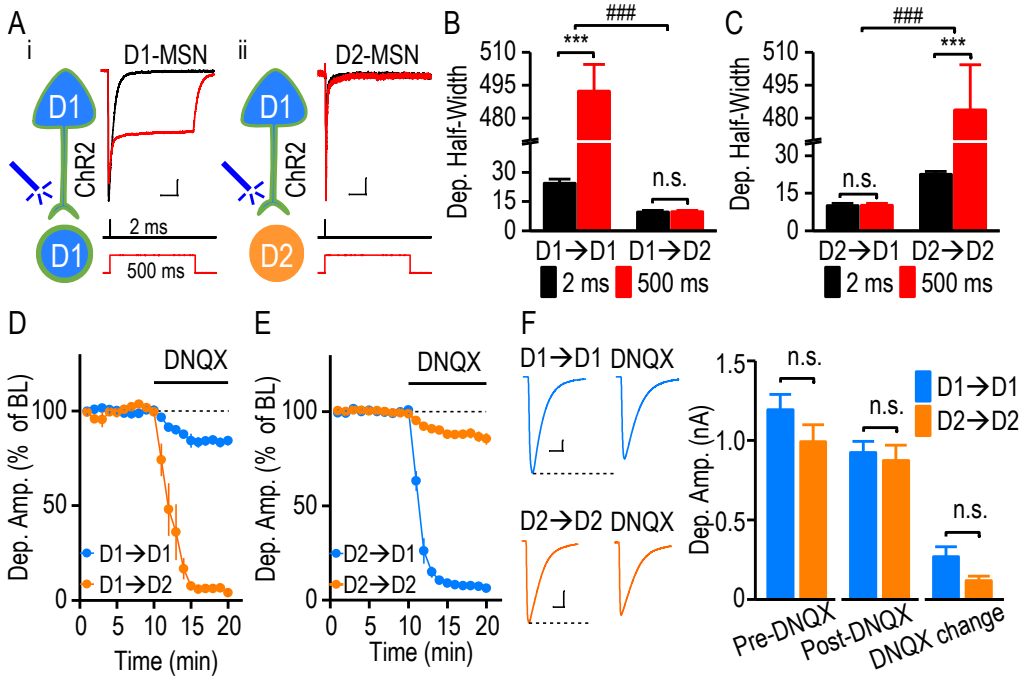

Supplementary Figure 1. Identification of MSNs and validation of DMS glutamatergic synapses. A, Left, an illustration showed the whole-cell recording at D1→D1 (i) and D1→D2 (ii) synapses in DMS slices from D1-Cre;Ai32 mice. Presynaptic D1R-expressing neurons and postsynaptic D1-MSNs, but not postsynaptic D2-MSNs, expressed ChR2. Right, representative traces indicated the membrane depolarization recorded in putative DMS D1-MSNs (i) and D2-MSNs (ii) in response to 2-ms (black) or 500-ms (red) light stimulation. Scale bars: 100 ms, 30 pA (A); 100 ms, 200 pA (B). Extended light stimulation caused significantly different responses in ChR2-expressing D1-MSNs and ChR2-negative D2-MSNs. **B-C,** Quantification of the half-width of 2-ms and 500-ms light-evoked responses in D1- and D2-MSNs from D1-Cre;Ai32 mice (B; n = 14 neurons, 6 mice [D1→D1]; 15 neurons, 6 mice [D1→D2]) and from D2-Cre;Ai32 mice (C; n = 14 neurons, 5 mice [D2→D1]; 13 neurons, 4 mice [D2→D2]). Note that a prolonged 500-ms light stimulation caused sustained ChR2-mediated direct

depolarization at D1→D1 and D2→D2 connections, but not at D1→D2 or D2→D1 synapses. $^{###}p < 0.001$, two-way RM ANOVA; $^{***}p < 0.001$, n.s. (not significant), $p > 0.05$, post hoc SNK test. **D-E**, Time course of light-evoked responses before and during bath application of DNQX in putative D1- and D2-MSNs from D1-Cre;Ai32 mice and D2-Cre;Ai32 mice. DNQX (10 μM) completely abolished light-evoked responses in D2-MSNs of D1-Cre;Ai32 mice (*D;* DNQX: 6.18 ± 1.29% of baseline, $t_{(5)} = 72.82$, $p < 0.001$) or in D1-MSNs of D2-Cre;Ai32 mice (*E*; DNQX: 7.73 ± 0.73% of baseline, $t_{(11)} = 126.51$, $p < 0.001$), indicating exclusive glutamatergic transmission at the D1→D2 and D2→D1 synapse. In contrast, DNQX caused a partial, but significant reduction of the light-evoked response in D1-MSNs of D1Cre;Ai32 mice (*D;* DNQX: 82.08 ± 2.73% of baseline, $t_{(10)} = 6.57$, $p < 0.001$) or in D2-MSNs of D2Cre;Ai32 mice (*E;* DNQX: 87.61 ± 2.39% of baseline, $t_{(9)} = 5.18$, $p < 0.001$). These results suggested that light stimulation triggered synaptic transmission, which was blocked by DNQX, and direct ChR2-mediated depolarization at the D1→D1 and D2→D2 synapse. n = 11 slices, 6 mice (*D;* D1→D1); 6 slices, 5 mice (*D;* D1→D2), 12 slices, 6 mice (*E;* D2→D1), and 10 slices, 8 mice (*E;* D2→D2). **F,** Left, sample traces of light-evoked responses in the absence and presence of DNQX at D1→D1 (top) and D2→D2 (bottom) synapses. Scale bars: 20 ms, 150 pA (top); 20 ms, 200 pA (bottom). Right, bar graphs compared the amplitudes of the light-evoked D1→D1 and D2→D2 responses in the absence and presence of DNQX, as well as the change induced by DNQX. n.s., not significant, $p > 0.05$, two-way RM ANOVA followed by post hoc SNK test. n = 12 neurons, 6 mice (D1→D1); 10 neurons, 8 mice (D2→D2).

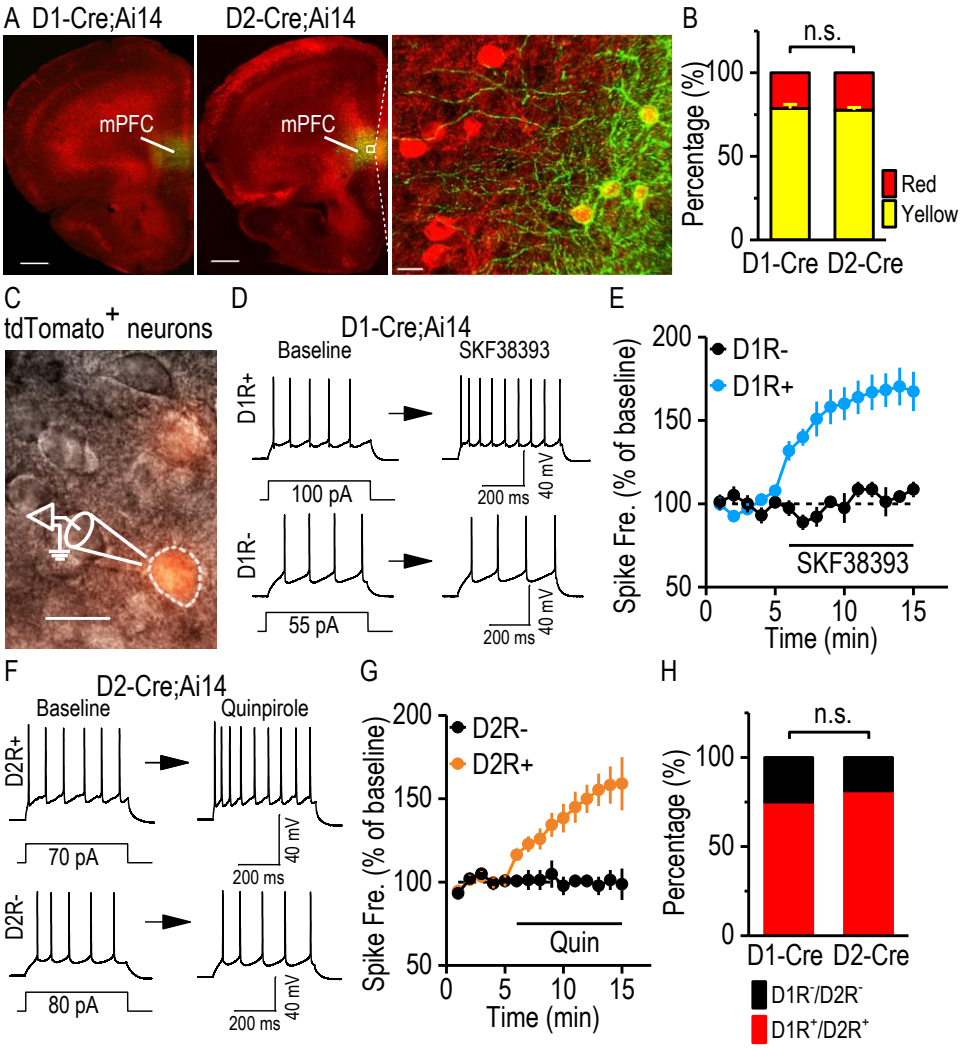

Supplementary Figure 2. Identical representation of dopamine receptor expression in D1-Cre and D2-Cre mice. To compare the reliability of Cre representation of D1R-expressing neurons in D1-Cre mice and of D2R-expressing neurons in D2-Cre mice, we crossed these mice with a tdTomato Cre reporter line, Ai14. **A-B**, Representative fluorescent image (A) and summarized data (B) for histological comparison. We infused AAV-CAG-Flex-GFP into the mPFC of D1-Cre;Ai14 (A; left) and D2-Cre;Ai14 mice (A; middle and right), and prepared coronal sections 10 days after the infusion. A high magnification image of the viral infusion site of a D2-Cre;Ai14 mouse showed co-

expression of GFP and tdTomato (A; right). Note that the D1R (D1-Cre mice) or D2R (D2-Cre mice) promotor drove Cre expression to turn on the viral-mediated GFP expression and Ai14-drived tdTomato expression. Thus, GFP represented neurons that currently expressed D1Rs or D2Rs, whereas tdTomato indicated neurons that historically (e.g., during development) and currently expressed these receptors. Summarized data (B) showed that the percentage of mPFC neurons co-expressing GFP and tdTomato (yellow) in cells that express tdTomato (red) did not differ between D1-Cre and D2-Cre mice. Scale bar: 500 μm (left and middle); 15 μm (right). n.s., $p > 0.05$, unpaired t test; n = 9 sections, 3 mice per group. **C-H,** Pharmacological comparison of Cre line efficiency. Red tdTomato-expressing ($tdTomato^+$) neurons in the mPFC of D1-Cre;Ai14 or D2-Cre;Ai14 mice were recorded in the current-clamp mode in the presence of DNQX (10 μM), APV (50 μM), and picrotoxin (100 μM) to block both excitatory and inhibitory synaptic transmission. A 500-ms current step was injected every minute to evoke firing in the absence and presence of a D1R or D2R agonist. Baseline and post-agonist firing frequencies were averaged from 1 to 5 min and from 11 to 15 min, respectively. Those neurons with ≥ 20% change in their post-agonist firing were operationally considered as D1R/D2R-expressing ($D1R^+$/$D2R^+$) neurons, and the remaining neurons were considered as D1R/D2R-negative ($D1R^-$/$D2R^-$) cells. Panel C showed representative DIC (grey) and fluorescent (red) images of $tdTomato^+$ pyramidal cells in the mPFC slice. Scale bar, 20 μm. Panel D showed sample traces of membrane potentials in the red $D1R^+$ (top) and $D1R^-$ (bottom) cells in response to a step current injection before (left, baseline) and during (right) bath application of a D1R agonist, SKF 38393 (20 μM) in the D1-Cre;Ai14 mice. Panel E showed the time course of averaged responses in evoked firing frequency before and during SKF38393

application in the red $D1R^+$ (blue) and $D1R^-$ (black) cells of D1-Cre;Ai14 mice. In 16 neurons from 4 D1-Cre;Ai14 mice, 12 of them were responsive to D1R agonist application. Sample traces (F) showed evoked firing of red $D2R^+$ (top) and $D2R^-$ (bottom) neurons before and during bath application of quinpirole (20 μM) in D2-Cre;Ai14 mice. Time course of averaged responses in evoked firing frequency before and during quinpirole application in the red $D2R^+$ (orange) and $D2R^-$ (black) cells of D2-Cre;Ai14 mice (G). In 16 neurons from 4 D2-Cre;Ai14 mice, 13 of them were responsive to D2R agonist application. Bar graph (H) summarized the percentage of $tdTomato^+$ neurons responded to the D1R/D2R agonist between D1-Cre;Ai14 and D2-Cre;Ai14 mice. D1-Cre and D2-Cre mice have identical reliability to represent the D1R-expressing neurons and D2R-expressing neurrons; n.s., $p > 0.05$; n = 16 neurons, 4 mice per group.

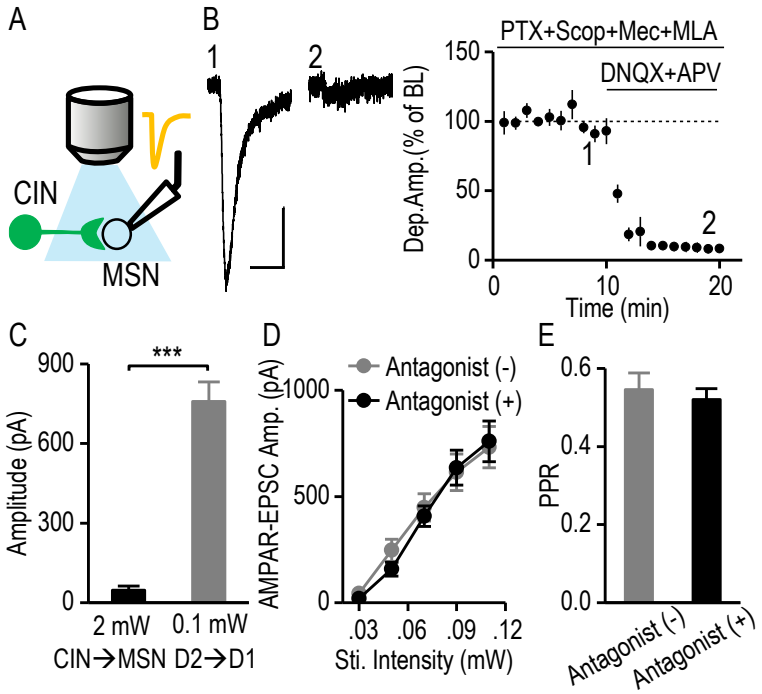

Supplementary Figure 3. The effect of DMS D2R-expressing cholinergic interneurons and dopaminergic terminals on glutamatergic transmission at the D2-D1 synapse during light stimulation. A, Schematic illustration showed light stimulation and recording arrangement in ChatCre;Ai32 mice. **B,** Left, sample traces of light-evoked CIN-mediated responses in MSNs in the absence (1) and presence (2) of glutamatergic transmission antagonists, DNQX (10 µM) and APV (50 µM). Scale bars: 40 ms, 5 pA. Right, the time course of light-evoked responses during bath application of DNQX and APV; $p < 0.05$, paired t test; n = 6 slices, 3 mice. **C,** Bar graph showed a significantly smaller glutamatergic transmission from CINs to MSNs than overall D2R-expressing neurons to D1-MSNs in the DMS; $^{***}p < 0.001$, unpaired t test; n = 8 neurons, 3 mice (CIN→MSN); 12 neurons, 6 mice (D2→D1). Grey bar graph indicated the data from Figure 1G as reference. Note that light stimulation intensity was 20-fold stronger in recordings of CIN→MSN than that in D2→D1. **D-E,** No detectable impact of acetylcholine

receptors and dopaminergic fibers on glutamatergic transmission at the D2→D1 connection during optical stimulation in the D2-Cre;Ai32 mice. The input-output relationship for AMPAR-EPSCs and PPR were measured in the absence and presence of a cocktail of antagonists of the D1R (SCH 23390, 10 μM), the D2R (sulpiride, 20 μM), the muscarinic acetylcholine receptor (scopolamine, 10 μM), and the nicotinic acetylcholine receptor (mecamylamine,10 μM; methyllycaconitine citrate, 50 nM). The antagonist cocktail did not significantly affect the input-output relationship for D2→D1 AMPAR-EPSCs (D; $F_{(1,84)} = 0.08$, $p > 0.05$; versus the same intensity in the group without antagonists, two-way RM ANOVA; n = 12 neurons, 6 mice [antagonists -]; 11 neurons, 4 mice [antagonists +]) or the PPRs (E; $t_{(22)} = 0.50$, $p > 0.05$, unpaired *t* test; n = 12 neurons, 4 mice per group). Grey line (D) and bar graph (E) indicated the data from water group in Figure 4A and Figure 4C as reference. PPR were evoked by two optical stimulations at a 100-ms interval.

REFERENCES

1. Klapoetke NC, Murata Y, Kim SS, Pulver SR, Birdsey-Benson A, Cho YK, et al. Independent optical excitation of distinct neural populations. Nat Methods. 2014;11:338-46.
2. Wei X, Ma T, Cheng Y, Huang CCY, Wang X, Lu J, et al. Dopamine D1 or D2 receptor-expressing neurons in the central nervous system. Addict Biol. 2018;23:569-84.
3. Cheng Y, Huang CC, Ma T, Wei X, Wang X, Lu J, et al. Distinct synaptic strengthening of the striatal direct and indirect pathways drives alcohol consumption. Biol Psychiatry. 2017;81:918-29.
4. Franklin KBJ and Paxinos G. The Mouse Brain in Stereotaxic coordinates. 3rd ed. Elsevier; 2007.
5. Wang J, Cheng Y, Wang X, Roltsch Hellard E, Ma T, Gil H, et al. Alcohol elicits functional and structural plasticity selectively in dopamine D1 receptor-expressing neurons of the dorsomedial striatum. J Neurosci. 2015;35:11634-43.
6. Cheng Y, Wang X, Wei X, Xie X, Melo S, Miranda RC, et al. Prenatal exposure to alcohol induces functional and structural plasticity in dopamine D1 receptor-expressing neurons of the dorsomedial striatum. Alcohol Clin Exp Res. 2018;42:1493-502.
7. Huang CCY, Ma T, Roltsch Hellard EA, Wang X, Selvamani A, Lu J, et al. Stroke triggers nigrostriatal plasticity and increases alcohol consumption in rats. Sci Rep. 2017;7:2501.
8. Ma T, Cheng Y, Roltsch Hellard E, Wang X, Lu J, Gao X, et al. Bidirectional and long-lasting control of alcohol-seeking behavior by corticostriatal LTP and LTD. Nat Neurosci. 2018;21:373-83.
9. Ma T, Barbee B, Wang X, and Wang J. Alcohol induces input-specific aberrant synaptic plasticity in the rat dorsomedial striatum. Neuropharmacology. 2017;123:46-54.
10. Ding J, Peterson JD, and Surmeier DJ. Corticostriatal and thalamostriatal synapses have distinctive properties. J Neurosci. 2008;28:6483-92.
11. Mateo Y, Johnson KA, Covey DP, Atwood BK, Wang HL, Zhang S, et al. Endocannabinoid actions on cortical terminals orchestrate local modulation of dopamine release in the nucleus accumbens. Neuron. 2017;96:1112-26 e5.